Carbohydrate Research 343 (2008) 2299–2307

Contents lists available at ScienceDirect

Carbohydrate Research

journal homepage: www.elsevier.com/locate/carres

^{13}C CP MAS NMR and crystal structure of methyl glycopyranosides

Katarzyna Paradowska [a], Tomasz Gubica [b], Andrzej Temeriusz [b,*], Michał K. Cyrański [b], Iwona Wawer [a]

[a] Department of Physical Chemistry, Faculty of Pharmacy, Medical University of Warsaw, Banacha 1, PL-02097 Warsaw, Poland
[b] Department of Chemistry, University of Warsaw, Pasteura 1, PL-02093 Warsaw, Poland

ARTICLE INFO

Article history:
Received 12 February 2008
Received in revised form 30 April 2008
Accepted 10 May 2008
Available online 23 May 2008

Keywords:
Crystal structure
^{13}C NMR analysis
Solid-state NMR
DFT GIAO calculations
Methyl glycopyranosides

ABSTRACT

The X-ray diffraction analysis, ^{13}C CP MAS NMR spectra and powder X-ray diffraction patterns were obtained for selected methyl glycosides: α- and β-D-lyxopyranosides (**1**, **2**), α- and β-L-arabinopyranosides (**3**, **4**), α- and β-D-xylopyranosides (**5**, **6**) and β-D-ribopyranoside (**7**) and the results were confirmed by GIAO DFT calculations of shielding constants. In X-ray diffraction analysis of **1** and **2**, a characteristic shortening and lengthening of selected bonds was observed in molecules of **1** due to anomeric effect and, in crystal lattice of **1** and **2**, hydrogen bonds of different patterns were present. Also, an additional intramolecular hydrogen bond with the participation of ring oxygen atom was observed in **1**. The observed differences in chemical shifts between solid state and solution come from conformational effects and formation of various intermolecular hydrogen bonds. The changes in chemical shifts originating from intermolecular hydrogen bonds were smaller in magnitude than conformational effects. Furthermore, the powder X-ray diffraction (PXRD) performed for **4**, **5** and **7** revealed that **7** existed as a mixture of two polymorphs, and one of them probably consisted of two non-equivalent molecules.

1. Introduction

^{13}C CP MAS NMR spectroscopy is a useful tool for structural studies of crystalline carbohydrates, as well as of insoluble polysaccharides. This technique complements X-ray crystallography since it can provide structural information on powders without the necessity of growing single crystals. However, the most important configurational and conformational data are obtained when combining solid-state NMR, high precision X-ray diffraction crystal structure analysis and theoretical quantum chemical methods.

The structural analysis of numerous crystalline derivatives of monosaccharides has been reported earlier,[1] but most of the studies did not include solid-state NMR spectroscopy results. Solid-state NMR is a valuable tool for studies of carbohydrates since the chemical shifts observed are sensitive to intermolecular hydrogen bonds, hydration, conformational effects and crystal packing. Therefore, it seemed worthwhile to look for the factors which affect these chemical shifts. Using ^{13}C CP MAS NMR spectroscopy, we examine a series of solid methyl glycopyranosides, namely three pairs of α and β anomers of: D-lyxo-, D-xylo- and L-arabino-pyranosides and also β-D-ribopyranoside, excluding methyl α-D-ribopyranoside which was earlier described as syrup[2] and therefore solid-state NMR measurements were impossible for this compound.

The assignment of signals in the ^{13}C CP MAS NMR spectra for the most popular saccharides like α- and β-D-glucopyranose was done by Pfeffer and Hicks in 1984.[3] Crystalline α and β anomers of methyl D-xylopyranoside were studied by ^{13}C CP MAS NMR by Taylor et al. in 1984[4] and by Bardet and Vincendon in 1994.[5] The complete ^{13}C chemical shift tensors were measured in single crystals of six methyl glycopyranosides (α- and β-D-galactopyranosides, α- and β-D-glucopyranosides, α-D-mannopyranoside and β-D-xylopyranoside) and interpreted with the aid of quantum chemical calculations of shielding constants.[6]

2. Results and discussion

2.1. Single crystal X-ray diffraction

Single crystals of methyl α- and β-D-lyxopyranosides (**1** and **2**) suitable for X-ray diffraction measurements were obtained by slow crystallization from ethyl acetate, or ethanol, respectively. The experimental data and structural refinement parameters are specified in Table 1. Molecular structures and atom numbering are shown in Figure 1, while selected bond lengths, bond angles and torsion angles and hydrogen bonds for **1** and **2** are given in Tables 2 and 3. The X-ray diffraction analysis of methyl α-D-lyxopyranoside (**1**) was performed earlier,[7] but currently presented analysis has significantly better structure refinement coefficient.

The molecules of **1** and **2** adopt $^4C_1$ conformations which are always slightly distorted due to crystal packing forces. The Cremer–Pople Θ puckering parameter[8] is equal to 0.584° for **1**

* Corresponding author. Fax: +48 22 822 5996.
E-mail address: atemer@chem.uw.edu.pl (A. Temeriusz).

0008-6215/$ - see front matter © 2008 Elsevier Ltd. All rights reserved.
doi:10.1016/j.carres.2008.05.015

Table 1
Crystal data and structure refinement for methyl α-D-lyxopyranoside (**1**) and methyl β-D-lyxopyranoside (**2**)

Compound	**1**	**2**
Molecular formula	$C_6H_{12}O_5$	$C_6H_{12}O_5$
Molecular weight	164.16	164.16
Crystal system	Orthorhombic	Orthorhombic
Space group	*P*2(1)2(1)2(1)	*P*2(1)2(1)2(1)
Z (molecules/cell)	4	4
$D_{calculated}$ (Mg/m^3)	1.422	1.409
Unit cell dimensions		
a (Å)	5.8090(4)	4.7212(3)
b (Å)	7.7102(5)	9.3171(4)
c (Å)	17.1173(13)	17.5888(9)
Volume ($Å^3$)	766.66(9)	773.69(7)
F(000) (e)	352	352
Wavelength (Å)	0.71073	0.71073
Absorption coefficient (mm^{-1})	0.125	0.124
Crystal size (mm^3)	0.1 × 0.05 × 0.05	0.1 × 0.05 × 0.05
Θ Range for data collection (°)	2.90–28.75	3.19–25.00
Limiting indices	$-7 \leqslant h \leqslant 7$ $-10 \leqslant k \leqslant 10$ $-22 \leqslant l \leqslant 21$	$-5 \leqslant h \leqslant 5$ $-11 \leqslant k \leqslant 11$ $-20 \leqslant l \leqslant 20$
Reflections collected	7143	5823
Independent reflections	1845 [R_{int} = 0.0384]	831 [R_{int} = 0.0236]
Data (restraints) parameters	1845/0/110	831/0/114
Goodness-of-fit on F^2	0.400	1.008
Final *R* indices [$I > 2\sigma(I)$]	R_1 = 0.0281; wR_2 = 0.0663	R_1 = 0.0225; wR_2 = 0.0507
R indices (all data)	R_1 = 0.0561; wR_2 = 0.0797	R_1 = 0.0283; wR_2 = 0.0518
Largest differences peak and hole $\Delta\rho$ ($e/Å^3$)	0.211 and −0.161	0.171 and −0.131

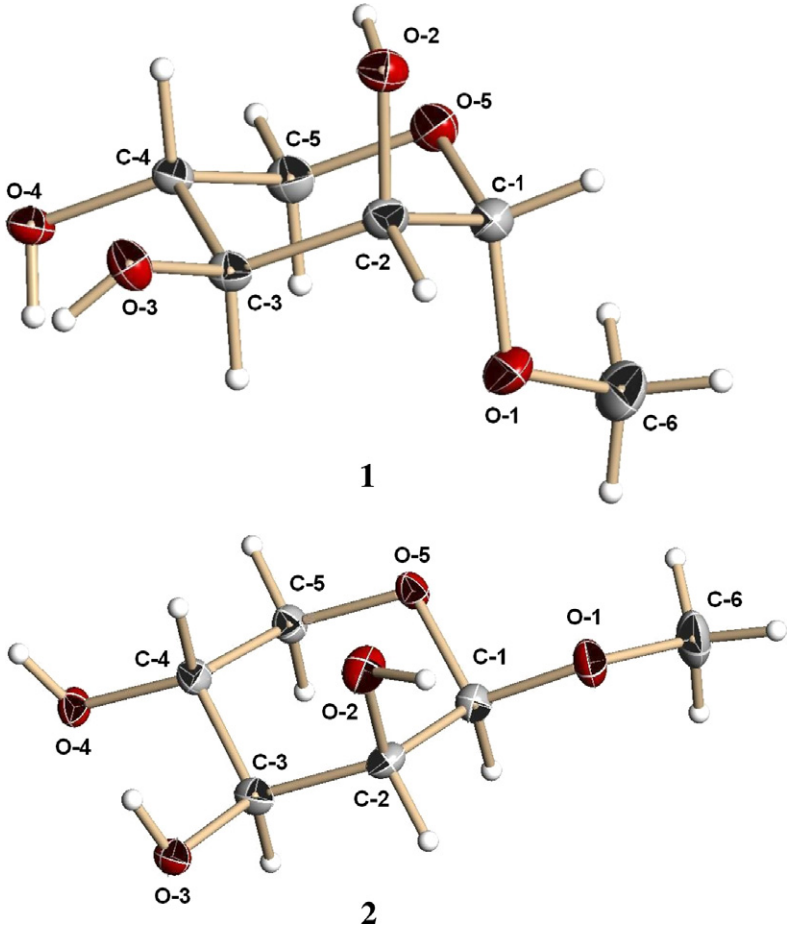

Figure 1. Molecular structure and atomic numbering of methyl α-D-lyxopyranoside (**1**) and methyl β-D-lyxopyranoside (**2**); the thermal ellipsoids are drawn at 50% probability.

Table 2
Selected bond lengths, bond angles and major torsion angles for methyl α-D-lyxopyranosides (**1**) and methyl β-D-lyxopyranosides (**2**)

Atoms	Compound	
	1	**2**
Bond lengths (Å)		
C-5–O-5	1.438 (2)	1.4340 (18)
O-5–C-1	1.426 (2)	1.4351 (19)
C-1–O-1	1.401 (2)	1.385 (2)
C-6–O-1	1.440 (2)	1.435 (2)
Bond angles (°)		
C-1–O-5–C-5	111.83 (13)	111.50 (12)
O-1–C-1–O-6	112.29 (15)	108.36 (13)
O-1–C-1–O-5	112.91 (15)	114.26 (13)
Torsion angles (°)		
O-5–C-1–O-1–C-6	66.46 (19)	−75.79 (17)
C-2–C-1–O-1–C-6	−172.35 (15)	164.40 (14)
O-1–C-1–O-5–C-5	58.58 (18)	−179.17 (13)

Table 3
Hydrogen bonds in methyl α-D-lyxopyranoside (**1**) and methyl β-D-lyxopyranoside (**2**)

Donor D-H	Acceptor A	*d* (D···H)	*d* (H···A)	∠DHA
Compound **1**				
O-2–H	O-5[a]	0.7792	2.5109	111.95
O-2–H	O-4	0.7792	2.0386	157.54
O-3–H	O-2	0.7684	1.9680	177.53
O-4–H	O-3	0.8005	1.9176	177.14
Compound **2**				
O-2–H	O-5	0.8711	1.8829	173.45
O-3–H	O-4	0.8367	1.9402	170.26
O-4–H	O-3	0.8565	1.8331	166.13

[a] Intramolecular hydrogen bond.

and 0.590° for **2**, while the other puckering parameters, Q and ϕ, are equal to 0.5°, 14.49° and 0.6°, 251.84° for **1** and **2**, respectively.

Both methyl α- and β-D-lyxopyranosides (**1**, **2**) crystallize in the $P2_12_12_1$ space group. An independent part of the unit cell is formed by four molecules of sugar in **1** and **2**. Due to the anomeric effect in **1** some differences in selected bond lengths between both anomers are observed. In **1**, the C-5–O-5 bond is slightly longer than that of C-1–O-5, but in **2**, the opposite situation is observed, that is, the C-1–O-5 bond is longer than that of C-5–O-5. Moreover, the glycosidic bond O-1–C-1 is shorter in **2** than in **1** (the difference in lengths is ca. 0.02 Å). The molecules in crystals of **1** and **2** are linked by hydrogen bonds; the common feature is that all three OH groups are hydrogen bond donors. The pattern of interactions is different, however, for **1** and **2** (Fig. 2) as donors and acceptors of hydrogen bonds are not the same for these compounds. In the crystals of **1** an intramolecular hydrogen bond is observed between hydroxyl group at C-2 atom and the ring oxygen atom of the same molecule, whilst in crystals of **2** this kind of hydrogen bonds is missing. An intramolecular hydrogen bonding, typical for crystals of **1**, is rarely observed in monosaccharides. The O-2–H···O-5 intramolecular hydrogen bond in **1** is slightly longer than others and shows large deviation (of ca. 68°) from linearity (Table 3).

The crystal structures of methyl glycopyranosides **3–7** were determined by X-ray diffraction and neutron diffraction or by these two methods (**5** and **7**). The crystal structures of methyl α-L-arabinopyranoside (**3**) and methyl β-L-arabinopyranoside (**4**) refined by X-ray diffraction measurements were reported elsewhere.[9] **3** and **4** adopt $^4C_1$ conformations with very small differences between their geometrical parameters. In both anomers of L-arabinopyranosides (**3** and **4**), the O-1–C-1 bond is the shortest, and the O–C-1–O valence angle is smaller in α as compared to β anomer. The hydrogen bond structure of α-anomer (**3**) consists of O-2–H···O-3 and O-3–H···O-2 infinite chains as well as the isolated bonds to the ring oxygen O-4–H···O-5. In **4**, there are only O-2–H···O-3, O-3–H···O-4 and O-4–H···O-2 bonds, that is, both the ring and glycosidic oxygen atoms are excluded from the hydrogen bond formation.

The crystal structures of methyl α- and β-D-xylopyranosides (**5** and **6**) are quite different. In particular, **5** crystallizes with two molecules in the asymmetric unit, while **6** has one molecule in the asymmetric unit. The neutron diffraction study of **5**[10] showed that it has four molecules per unit cell. The X-ray diffraction data[11] indicate that the only significant conformational difference between two independent molecules of **5** is in the dihedral angle O-5–C-1–O-1–CH_3 (the difference of ca. 6°). In the crystals of **6**, the bond to the ring oxygen atom O-2–H···O-5 is the longest, as it would be expected, and the donor-only bond O-4–H···O-3 is shorter than the donor–acceptor bond O-3–H···O-2.

The structure of orthorhombic crystal of methyl β-D-ribopyranoside (**7**), the only known crystallographic form of **7**, was refined using both X-ray and neutron-diffraction methods.[12] Compound **7** crystallized with $P2_12_12_1$ space group with one molecule in the asymmetric unit ($^1C_4$ conformation). The crystal structure of **7** revealed four intermolecular hydrogen bonds and one intramolecular hydrogen bond per molecule. Each hydroxyl group of this compound was both donor and acceptor in the hydrogen bonding scheme. The intramolecular hydrogen bond in **7** was placed between the syndiaxially oriented O-2–H and O-4, with distance between O···O atoms of 2.768 Å. Intermolecular and intramolecular interactions in **7** excluded the ring and glycosidic oxygen atoms.

2.2. ^{13}C CP MAS NMR spectroscopy

The series of seven methyl glycopyranosides (**1–7**), was studied by means of solid-state ^{13}C CP MAS NMR spectroscopy, thus complementing the crystal structures of these compounds. The cross-polarization was effective, as frequently occurs in carbohydrates, since the maximum intensity of signals was achieved with contact time of 1.5 ms and the spectra of reasonably good quality were obtained when accumulating ca. 200–300 scans. The ^{13}C CP MAS NMR spectra of **3**, **4** and **7** are illustrated in Figure 3. Close correlations between XRD and MAS NMR data are expected for both lyxopyranosides **1** and **2** because the X-ray and NMR studies were performed using the same samples in both techniques (crystals were powdered for MAS NMR measurements).

The chemical shifts for solids and solutions (in DMSO-d_6) and the differences between solution and solid state $\Delta = \delta_{solution} - \delta_{solid} > 1$ ppm for **1–7** are given in Table 4. Since solid-state techniques, such as dipolar diphase or short contact pulse sequences, are less helpful in distinguishing C–H resonances of carbohydrate than solution techniques. Therefore, the chemical shifts were assigned mainly by comparison with solution data and the calculated shielding constants. The dependence of solid-state chemical shifts on intermolecular interactions result from the close proximity of neighboring molecules in the crystals, although it should also be kept in mind that the intramolecular interactions associated with conformational effects can also produce different chemical shifts.

To assess the conformational effects, for example, freezing the rotation around glycosidic bond, the rotation of OH groups or the differences in the dihedral angle O-5–C-1–O-1–CH_3, the comparison of chemical shifts in solid state and solution has been made which allows detection of the rigid and flexible structural fragments of the molecules. The flexible fragments should exhibit larger shielding changes than the rigid ones. It is expected that for a rigid system such as pyranosidic ring of the chair-like conformation in **1–7**, only the OCH_3 group at anomeric carbon C-1 can undergo reorientation. As shown in Table 4, the differences in

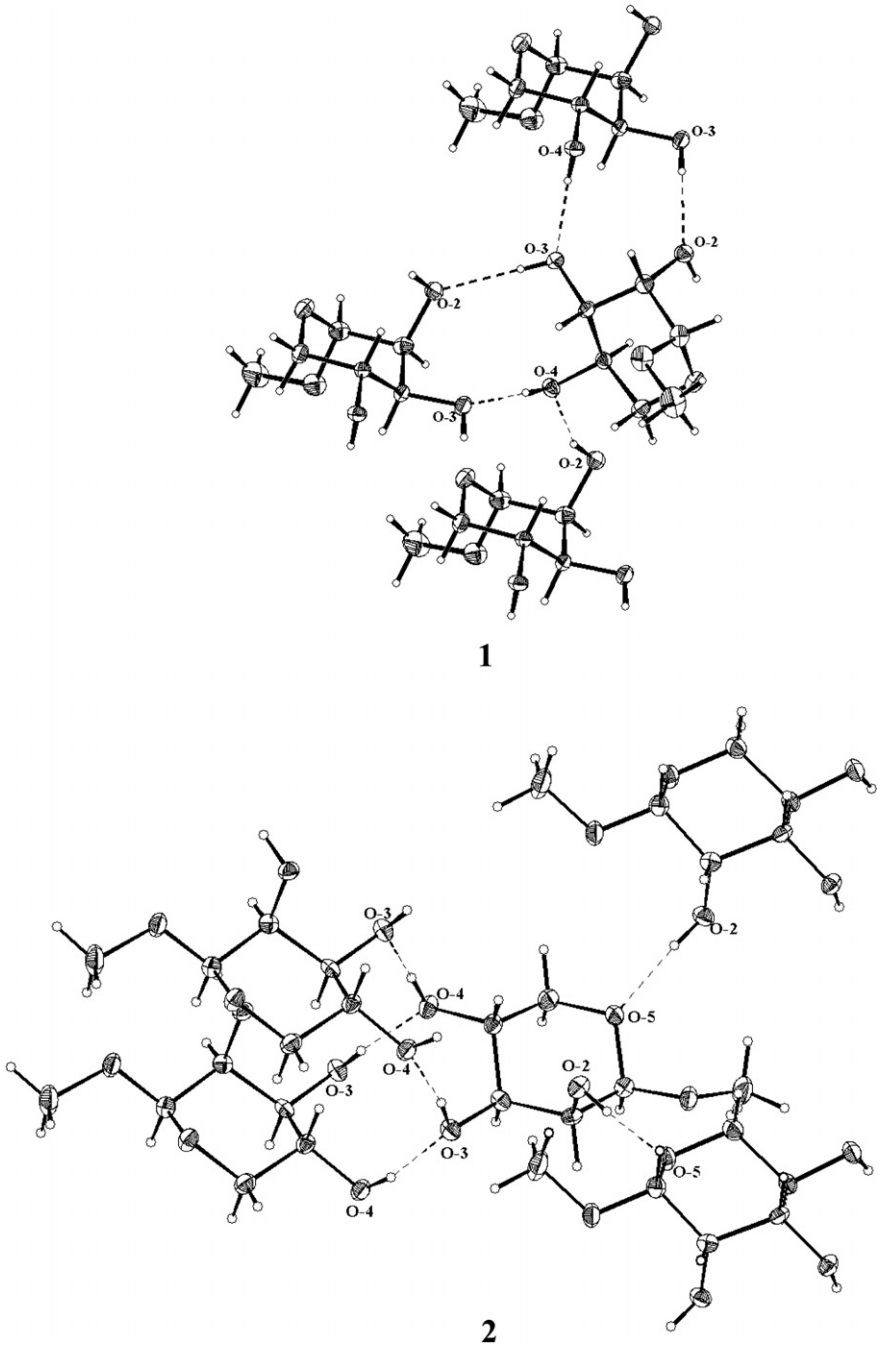

Figure 2. Crystal packing of methyl α-D-lyxopyranoside (**1**) and methyl β-D-lyxopyranoside (**2**); the hydrogen bonding are indicated in dashed lines.

chemical shifts are indeed significant for C-1 and OCH_3. For these carbon atoms deshielding frequently occurs in solid state.[13,14] The shifts other than that are less sensitive to conformational effects.

In solid state, the OH groups of **1**–**7** are involved in hydrogen bond donor-and-acceptor or single-donor interactions. Therefore, the differences in chemical shifts for all carbon atoms bearing the OH group, that is, C-2, C-3 and C-4, in solution and solid state can be related, in the first approximation, to the formation of intermolecular hydrogen bonds. Some increase in carbon shielding could be expected upon formation of C–OH···O bonds (as suggested by the calculated shielding constants). A hydrogen bonding pattern in which only C–OH groups participate in intermolecular interactions (ring and glycosidic oxygen atoms are excluded) is realized in **1** and **4**.[9]

The chemical shifts of carbon atoms in solid-state NMR spectroscopy, for **1** (Table 4), are either the same as for solution counterparts (C-2, C-4) or smaller (for C-3 and C-5 Δ = 2.2 and 2.7 ppm, respectively). Surprisingly, the largest differences between solid state and solution NMR studies of **1** appear for C-1 (−5.9 ppm) and OCH_3 (3 ppm) (Table 4). Taking into account that neither ring oxygen atom O-5 nor OCH_3 participate in intermolecular hydrogen bonds, such large effects result rather from conformational changes than from the intermolecular interactions. For β anomer (**2**), the differences in Δ parameters are smaller (−2.3 to 1.7 ppm) than for α anomer (**1**). In contrast to **1**, in the crystal of **2** intermolecular hydrogen bonds involve the ring oxygen atom O-5. Deshielding of C-5 carbon atom (−2.3 ppm) can be explained by the formation of C-5–H···O weak intermolecular interaction.

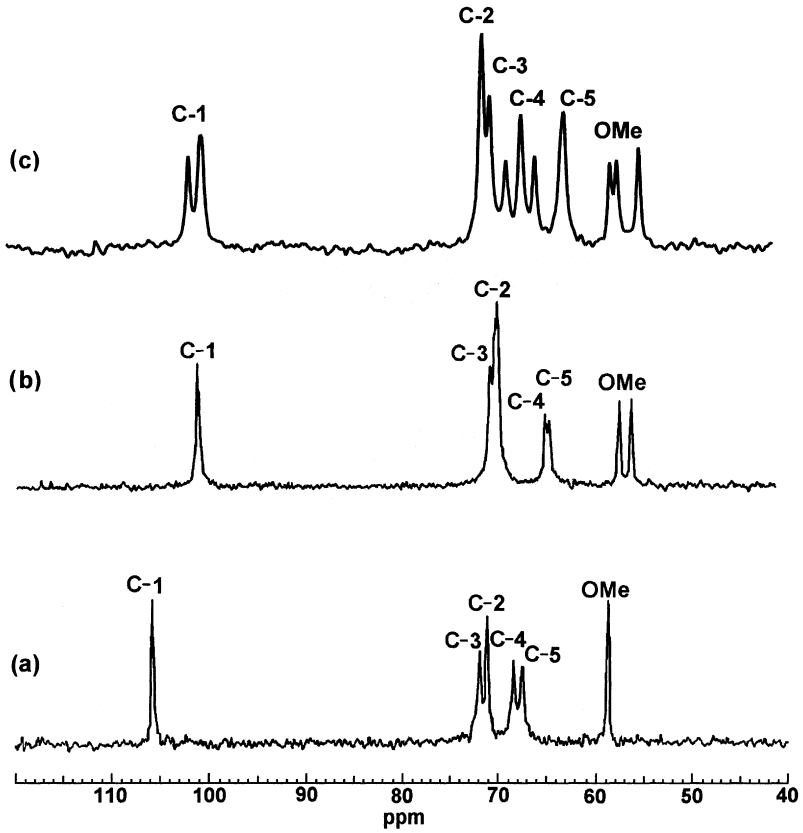

Figure 3. ^{13}C CP MAS NMR spectra of (a) methyl α-L-arabinopyranoside (**3**), (b) methyl β-L-arabinopyranoside (**4**) and (c) methyl β-D-ribopyranoside (**7**); rotational speed of 8 kHz.

Table 4
^{13}C NMR chemical shifts for solid methyl glycopyranosides **1–7**, for DMSO-d_6 solutions (in parentheses) and the differences $\Delta = \delta_{solution} - \delta_{solid} > 1$ ppm

Compound	C-1	C-2	C-3	C-4	C-5	OCH_3
1	100.8 (94.9) −5.9	71.6 (71.1)	71.6 (73.8) 2.2	68.2 (67.9)	62.6 (65.3) 2.7	53.9 (56.9) 3.0
2	103.7 (102.0) −1.7	71.8 (70.4) −1.4	72.5 (71.6) −0.9	66.0 (67.7) 1.7	65.6 (63.3) −2.3	56.9 (55.9) −1.0
3	105.7 (105.1)	71.2 (71.8)	72.0 (73.0) 1.0	68.4 (69.4) 1.0	67.5 (67.3)	58.7 (57.1)
4	100.9 (101.0)	69.2 (69.4)	70.0 (69.9)	69.2 (70.0)	64.1/63.7 (63.8)	56.5/55.2 (56.3) −/1.1
5	101.7/100.3 (100.6) −1.1/−	73.5/72.6 (72.3) −1.2/−	74.5 (74.3)	71.6/69.8 (70.4) −1.2/−	62.7/61.7 (62.0)	57.9/55.4 (56.0) −1.9/−
6	105.1 (105.1)	73.4 (74.0)	79.1 (76.9) −2.2	70.4 (70.4)	67.6 (66.3) −1.4	58.3 (58.3)
7	101.0/99.7 (101.8) −/2.1	70.3 (70.6)	69.5/67.8 (68.4) −1.1/−	66.3/64.8 (67.3) −/2.5	61.8 (63.5) 1.7	57.0/56.3/54.0 (55.1) −1.9/−1.2/1.1

The minor difference in the chemical shift of carbon atoms for **3** and **4** was observed, except for splitting the resonances of **4**. The differences of Δ parameters observed for C-2, C-3 and C-4 are smaller than 1 ppm, and it could be a result of formation of intermolecular hydrogen bonds in the solid state (C-2–OH···O-3, C-3–OH···O-2, C-4–OH···O-5). The splitting of resonances into doublets (Fig. 3b) could indicate, however, that **4** forms two polymorphs. The chemical shifts of methyl group are particularly sensitive to the crystallographic non-equivalence of mixture of polymorphs. In the spectrum of **4**, the resonances of OMe are separated by 1.3 ppm, the separation of C-5 signals is 0.4 ppm and C-1 appears as singlet at 100.9 ppm. These results suggest that such splitting

of resonances of **4** could result from the polymorphism of **4** or from two non-equivalent molecules in the crystal unit cell of **4**. It will be shown in the next section that this dilemma can be resolved by the PXRD results.

The ^{13}C CP MAS NMR spectra of methyl α- and β-D-xylopyranosides (**5** and **6**) reflected quite different crystal structures. Compound **6** crystallizes with one molecule in the asymmetric unit, while the **5** has two independent molecules (11 signals in the ^{13}C CP MAS NMR spectrum). The only larger conformational difference between two crystalline forms of **5** is in the dihedral angle O-5–C-1–O-1–CH_3, and the largest differences in ^{13}C CP MAS chemical shifts appear for C-1 (1.4 ppm) and OCH_3 (2.5 ppm). The comparison of chemical shifts in solid state and in solution reveals that the upfield component of the doublets is close to the solution value, whereas the low-field one is shifted by 1.1–1.9 ppm versus the solution value. This set of resonances may represent a molecule with larger differences in geometry from that found in solution. In **6** there is one molecule in the crystal unit, as indicated by the single resonance for particular carbon atoms in a molecule. For **6**, the differences in Δ are only significant for C-3 and C-5 (−2.2 and −1.4 ppm, respectively).

The most interesting NMR results were obtained for methyl β-D-ribopyranoside (**7**). In the ^{13}C CP MAS NMR spectrum of **7** (Fig. 3c), the resonances of C-1, C-3, C-4 and OCH_3 are split into triplets indicating the presence of three different molecules. However, the neutron-diffraction data[12] for **7** showed one molecule in the asymmetric unit of the crystal. The possible interpretation of this phenomenon will be discussed in the section that follows.

2.3. Powder X-ray diffraction

The confirmation of crystal structures and NMR data for **4**, **5** and **7** was obtained from the powder X-ray diffraction patterns. The splitting of resonances in the spectrum of **4** could indicate that the studied sample forms two polymorphs. And indeed, powder X-ray diffraction patterns for **4** (Fig. 4) indicated the presence of two polymorphs, monoclynic[15] and orthorhomic[9] ones.

As described in Section 2.1, **5** has two independent molecules in the crystal unit cell. Moreover, 11 signals in the ^{13}C CP MAS NMR were found in the spectrum of **5** (Section 2.2). Therefore, the PXRD measurements were performed for **5** in order to verify the suggestion that such resonance splitting comes from two non-equivalent molecules, and not from two polymorphs. The experimental powder X-ray diffraction pattern of **5** (Fig. 5) closely matches that calculated from single crystal X-ray diffraction refinement in 2θ angles. This confirms the presence of a particular crystal form in the sample. The observed small variation in the relative peak intensities is subjected to preferred orientation effects.

The diffraction pattern of **7** (Fig. 6) confirmed the presence of orthorhombic[12] and another unknown crystal form of methyl β-D-ribopyranoside. So, the splitting of resonances in ^{13}C CP MAS NMR spectrum of **7** seems to be caused by at least two polymorphs existing in the sample. This reasoning leads to another important conclusion. If **7** exists as a mixture of two polymorphs, then the unknown polymorph should possess two non-equivalent molecules in the crystallographic unit cell, because of the splitting of resonances into triplets in CP MAS NMR spectrum.

2.4. GIAO CPHF calculations of shielding constants

Since chemical shifts measured for solid samples reflect intermolecular interactions, the shielding of C-2, C-3 and C-4 (bearing OH groups) should be affected by hydrogen bonding. This idea prompted us to study, in greater detail, the effect of hydrogen bonding using theoretical methods. The basis set B3LYP/6-31G* was sufficiently large to yield energies and geometrical parameters for sugars and their derivatives, especially associates with COH···OH_2 and/or CO···HOH bonds.

The crystal structure of **1** was used as a starting point for calculations. Next, the associates with water molecules were calculated

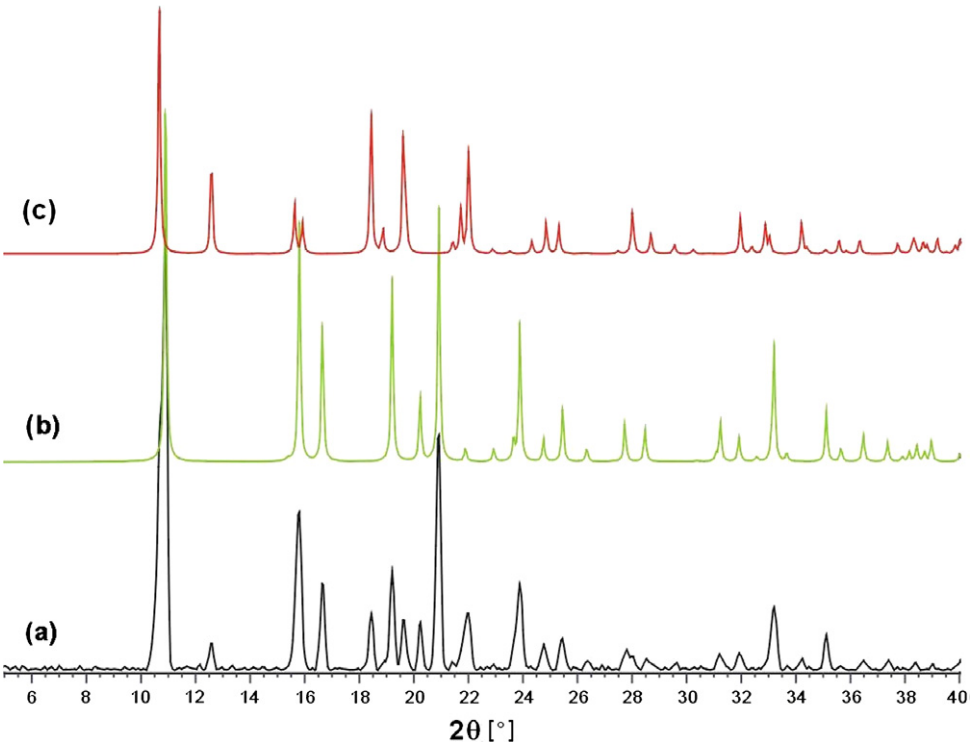

Figure 4. Observed PXRD pattern of **4** (a); compared with the theoretically calculated pattern of monoclinic[15] (b) and orthorhombic[9] (c) polymorphs of methyl β-L-arabinopyranoside.

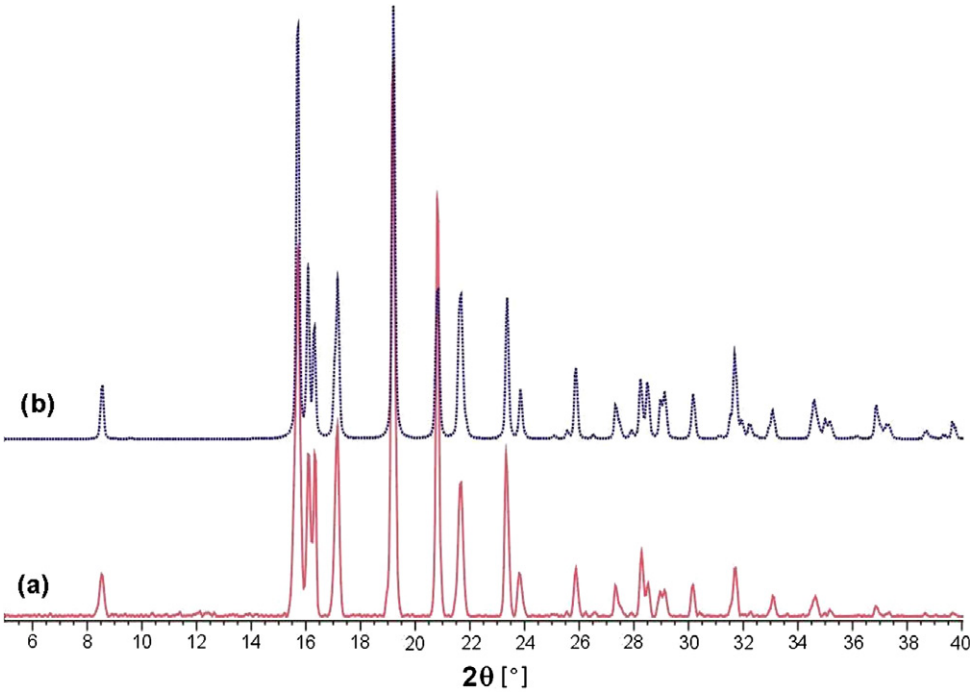

Figure 5. Observed PXRD pattern of **5** (a); compared with the theoretically calculated pattern of methyl α-D-xylopyranoside[10] (b).

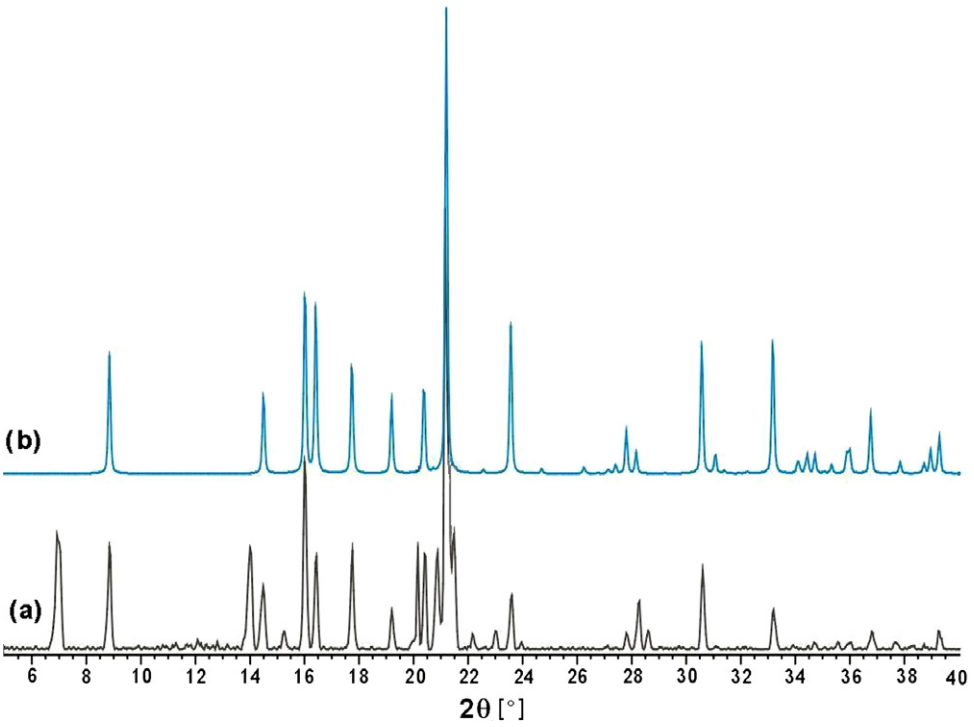

Figure 6. Observed PXRD pattern of **7** (a); compared with the theoretically calculated pattern of methyl β-D-ribopyranoside[12] (b).

to consider the effects of intermolecular hydrogen bond formed by particular OH groups (Table 5). Examination of the conformational energies of the minimized structures indicates that hydrogen bonds stabilize the structures of **1**; each added interaction with water decreased total energy of the hydrate. Figure 7 shows the correlation plot of the computed shielding constants versus the experimental CP MAS chemical shifts (shielding constant for TMS methyl carbons and glycine carbonyl carbon were included).

The differences for C-2, C-3 and C-4 in calculated shielding constants were expected due to the effects of hydrogen bonding, and indeed, the theoretical values of σ for hydrates differed by 1–3 ppm from that of an isolated molecule. The largest

Table 5
The GIAO CPHF calculated shielding constants for isolated molecule of methyl α-D-lyxopyranoside (**1**) and its hydrogen bonded hydrates

Type of H-bond	Energy[a] (kcal/mol)	C-1	C-2	C-3	C-4	C-5	OCH_3	R^{2b}
Isolated molecule	−54427.14	84.66	115.18	113.92	119.60	125.83	137.64	0.9935
C-2–O···HOH ($1 \times H_2O$)	−62033.78	85.60	115.49	114.20	119.42	126.01	137.62	0.9929
C-3–O···HOH ($1 \times H_2O$)	−62033.89	84.58	115.59	115.57	119.86	125.98	137.62	0.9972
C-4–OH···OH_2 C-4–O···HOH ($2 \times H_2O$)	−69531.80	84.71	115.18	114.42	120.88	126.90	137.68	0.9942
C-2–O···HOH C-4–O···HOH ($2 \times H_2O$)	−69529.13	85.74	115.44	114.72	119.82	126.62	137.59	0.9941
C-2–O···HOH C-3–O···HOH C-4–O···HOH ($3 \times H_2O$)	−77026.66	85.66	115.82	116.20	120.08	126.69	137.61	0.9972
C-2–O···HOH C-3–O···HOH C-4–OH···OH_2 ($3 \times H_2O$)	−77028.13	85.45	116.00	115.46	120.22	126.66	137.70	0.9966
C-2–O···HOH C-3–O···HOH × 2 ($3 \times H_2O$)	−77031.39	85.46	116.74	115.30	119.57	126.17	137.67	0.9961

[a] $E_{water} = -7492.69$ kcal/mol.
[b] Shielding constant: $\sigma = 192.25$ ppm for TMS methyl carbon atoms and σ (C=O) = 27.21 ppm, $\delta = 176.03$ ppm for glycine used as an external reference.

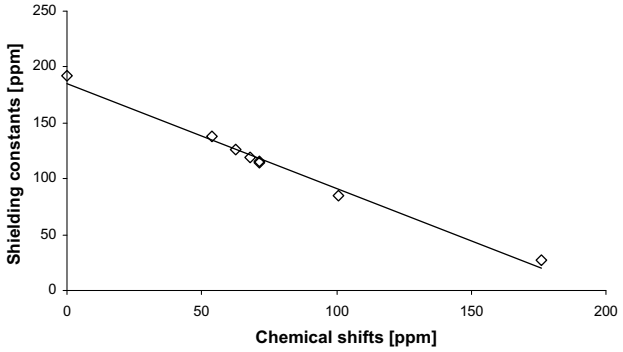

Figure 7. Correlation between theoretical shielding constants and experimental values of ^{13}C chemical shifts for isolated molecule of methyl α-D-lyxopyranoside (**1**), (including data for TMS and glycine C=O).

discrepancies are observed for C-3. The inspection of the crystal structure showed that an approach of water molecule to the axially oriented C-4–OH hydroxyl group results in slight differences (up to 2°) of the O-5–C-1–O-1–CH_3 torsional angle, which influences the shielding parameters of the neighboring carbon atoms.

The studies of methyl α-D-lyxofuranoside by DFT methods showed[17] that each hydrogen bond increased the stability of the furanoside by approximately 2.2 kcal/mol. DFT calculations at the B3LYP/6-31G* level for methyl α-D-ribofuranoside[18] and methyl α-D-arabinofuranoside[19] have been reported. The procedures have been proposed for selection of starting geometries with staggered exocyclic bonds and the least serious eclipsing of ring substituents (exocyclic rotamers are chosen to avoid internal hydrogen bonds; for the structures with no hydrogen bonds avoidance of eclipsing is the dominant factor).

The results of DFT calculations for **1** showed that both conformational and hydrogen bonding effects produce significant chemical shift changes, but it is difficult to separate them. The latter effect seemed to be smaller than the former one.

3. Experimental

3.1. Materials

Methyl aldopyranosides were prepared by methanolysis of the corresponding aldoses with anhydrous MeOH in presence of Amberlite IR-120 resin, or HCl. The derivatives obtained were characterized by physical constants in good agreement with the literature values (Table 6).

3.2. Physical measurements

The ^{13}C NMR spectra for DMSO-d_6 solutions were recorded on a UNITY-500 spectrometer, the 2D experiments were run using standard VARIAN software. Cross polarization magic angle spinning solid-state ^{13}C NMR spectra were recorded at 100.1 MHz on Bruker DRX-400 MHz spectrometer. Powder samples were spun at 8 kHz in 4 mm ZrO_2, contact time of 4–5 ms, repetition time of 8 s and spectral width of 25 kHz were used for accumulation of 200–500 scans. Chemical shifts were calibrated indirectly through the glycine CO signal recorded at 176.0 ppm, relative to TMS.

The X-ray measurement of **1** and **2** was performed at 100 (2) K on a KUMA CCD κ-axis diffractometer with graphite-monochromated MoKα radiation (0.71073 Å). The crystals were positioned at 62.25 mm from the KM4CCD camera; 1000 and 1200 frames were measured at 0.6° and 0.5° intervals on a counting time of 35 s and 25 s (for **1** and **2**, respectively). Data reduction and analysis were carried out with the KUMA Diffraction programs. The data were corrected for Lorentz and polarization effects but no absorption correction was applied. The structure was solved by direct methods[27] and refined by using SHELXL.[28] The refinement was based on F^2 for all reflections except for those with very negative F^2. The weighted R factor, wR and all goodness-of-fit S values are based on F^2. The non-hydrogen atoms were refined anisotropically. The hydrogen atoms were located from a difference map and were refined isotropically. The atomic scattering factors were taken from the International Tables.[29] Crystal data together with the data collection and structure refinement details are listed in Table 1.

Table 6
Physical data for compounds **1–7**

	Compound	Mp °C (lit.)	$[\alpha]_D$ (°) in water (lit.)
1	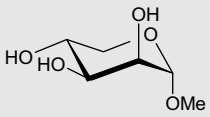	108–109 (108)[20]	+59.8 (+59.4)[20]
2	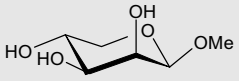	118 (118)[21]	−126 (−128.1)[21]
3	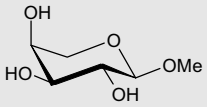	131–132 (131)[22]	+17.3 (+17.3)[22]
4	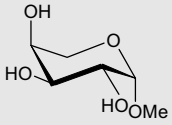	169–171 (169)[20]	+245 (+245.5)[20]
5	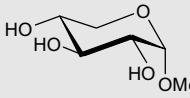	90–91 (90)[24]	+150 (+153.7)[24]
6	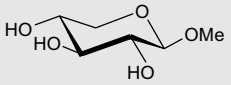	156–157 (157)[23]	−64.5 (−65.5)[23]
7	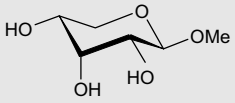	82–83 (82–83)[25]	−103 (−105)[26]

The powder X-ray diffraction patterns of **4**, **5** and **7** were recorded on a Seifert HZG-4 automated diffractometer using Cu$K\alpha_{1,2}$ radiation (1.5418 Å). The data were collected in the Brag–Brentano ($\theta/2\theta$) horizontal geometry (flat reflection mode) between 5° and 40° (2θ) in 0.04° steps, at 5° s step^{-1}. The optic of the HZG-4 diffractometer was a system of primary Soller slits between the X-ray tube and the fixed aperture slit of 2.0 mm. One scattered-radiation slit of 2 mm was placed after the sample, followed by the detector slit of 0.2 mm. The X-ray tube operated at 40 kV and 40 mA.

Powder XRD patterns were simulated from single crystal data using the program MERCURY.[30]

3.3. Theoretical calculations

The shielding constants were calculated using the GIAO CPHF approach implemented in GAUSSIAN 98[16] package with the standard 6-31G** basis set on molecular geometry taken from the semi-empirical calculation by PM3 method using HYPERCHEM 5.02.[31]

Supplementary data

Full crystallographic details have been deposited in Cambridge Crystallographic Data Centre. These data may be obtained, on request, from The Directory, Cambridge Crystallographic Data Centre, 12 Union Road, Cambridge CB2 1EZ, UK (fax: +44-1223-336033; e-mail: deposit@ccdc.cam.ac.uk or www: http://www.csdc.cam.ac.uk). Deposition numbers: CCDC 676558 (**1**) and 676559 (**2**).

Acknowledgements

Financial support from the Medical University of Warsaw (FW-28/N/2006) and Warsaw University (BST-112152) is gratefully acknowledged. The X-ray measurements were performed in the Crystallographic Unit of the Physical Chemistry Laboratory at the Department of Chemistry of the Warsaw University. The authors are grateful to Dr. Andrzej Ostrowski (Department of Chemistry, Technical University of Warsaw) for recording the powder X-ray diffraction patterns and for helping to interpret them.

References

1. Jeffrey, G. A.; Saenger, W. *Hydrogen Bonding in Biological Structures*; Springer: Berlin, 1991.
2. Barker, G. R.; Smith, D. C. C. *J. Chem. Soc.* **1954**, 2151–2153.
3. Pfeffer, P. E.; Hicks, K. B. *J. Carbohydr. Chem.* **1984**, *3*, 197–217.
4. Taylor, M. G.; Marchessault, R. H.; Perez, S.; Stephenson, P. J.; Fyfe, C. A. *Communication* **1984**, 270–273.
5. Bardet, M.; Vincendon, M. *Carbohydr. Res.* **1994**, *264*, 135–140.
6. Liu, F.; Phung, C. G.; Alderman, D. W.; Grant, D. M. *J. Am. Chem. Soc.* **1996**, *118*, 10629–10634.
7. Evdokimov, A. G.; Frolow, F. *Acta Crystallogr., Sect. C* **1996**, *52*, 3218–3219.
8. (a) Cremer, D.; Pople, J. A. *J. Am. Chem. Soc.* **1975**, *97*, 1354–1358; (b) Cremer, D. *Acta Crystallogr., Sect. B* **1984**, *40*, 498–500.
9. Takagi, S.; Jeffrey, G. A. *Acta Crystallogr., Sect. B* **1978**, *34*, 1591–1596.
10. Takagi, S.; Jeffrey, G. A. *Acta Crystallogr., Sect. B* **1978**, *34*, 3104–3107.
11. Takagi, S.; Jeffrey, G. A. *Acta Crystallogr., Sect. B* **1977**, *33*, 3033–3040.
12. James, V. J.; Stevens, J. D.; Moore, F. H. *Acta Crystallogr., Sect. B* **1978**, *34*, 188–193.
13. Wawer, I.; Piekarska-Bartoszewicz, B.; Temeriusz, A. *Carbohydr. Res.* **1995**, *267*, 167–176.
14. Temeriusz, A.; Piekarska-Bartoszewicz, B.; Wawer, I. *Carbohydr. Res.* **1997**, *304*, 335–340.
15. Il'in, S. G.; Reshetnyak, M. V.; Evtushenko, E. V. *Chem. Nat. Compd.* **1986**, *21*, 566–570.
16. Frisch, M. J.; Trucks, G. W.; Schlegel, B.; Scuseria, G. E.; Robb, M. A.; Cheeseman, J. R.; Zakrzewski, V. G.; Montgomery, J. A., Jr.; Stratmann, R. E.; Burant, J. Dapprich, C. S.; Millam, J. M.;. Daniels, A. D.; Kudin, K. N.; Strain, M. C.; Farkas, O.; Tomasi, J.; Barone, V.; Cossi, M.; Cammi, R.; Mennucci, B.; Pomelli, C.; Adamo, C.; Clifford, S.; Ochterski, J.; Petersson, G. A.; Ayala, P. Y.; Cui, Q.; Morokuma, K.; Malick, D. K.; Rabuck, A. D.; Raghavachari, K.; Foresman, J. B.; Cioslowski, J.; Ortiz, J. V.; Baboul, A. G.; Stefanov, B. B.; Liu, G.; Liashenko, A.; Piskorz, P.; Komaromi, I.; Gomperts, R.; Martin, R. L.; Fox, D. J.; Keith, T.; Al-Laham, M. A.; Peng, C. Y.; Nanayakkara, A.; Gonzalez, C.; Challacombe, M.; Gill, P. M. W.; Johnson, W. B.; Chen, W.; Wong, M. W.; Andres, J. L.; Gonzalez, C.; Head-Gordon, M.; Replogle, E. S.; Pople, J. A. GAUSSIAN 98. Revision A.7. Gaussian: Pittsburgh, PA, 1998.
17. Evdokimov, A.; Gilboa, A. J.; Koetzle, T. F.; Klooster, W. T.; Schultz, A. J.; Mason, S. A.; Albinati, A.; Frolow, F. *J. Phys. Chem.* **2000**, *104*, 5291–5297.
18. Cloran, F.; Carmichel, I.; Serianni, A. S. *J. Phys. Chem. A* **1999**, *103*, 3783–3795.
19. Gordon, M. T.; Lowary, T. L.; Hadad, C. M. *J. Am. Chem. Soc.* **1999**, *121*, 9682–9692.
20. Bennett, M.; Gill, G. B.; Pattenden, G.; Shuker, A. J.; Stapleton, A. *J. Chem. Soc., Perkin Trans. 1* **1991**, 929–937.
21. Isbell, H. S.; Frush, H. L. *J. Res. Nat. Bur. Stand. (US)* **1940**, *24*, 125–151.
22. Hudson, C. S. *J. Am. Chem. Soc.* **1926**, *47*, 265–268.
23. Weiges, K.; Haremsa, S.; Maurer, W. *Carbohydr. Res.* **1987**, *164*, 453–458.
24. Dale, J. K.; Hudson, C. S. *J. Am. Chem. Soc.* **1930**, *52*, 2534–2537.
25. Durette, P. L.; Horton, D. *Carbohydr. Res.* **1971**, *18*, 403–418.
26. Pedersen, C.; Fletcher, H. G., Jr. *J. Am. Chem. Soc.* **1960**, *82*, 945–947.
27. Sheldrick, G. M. *Acta Crystallogr., Sect. A* **1990**, *46*, 467–473.
28. Sheldrick, G. M. SHELXL*93. Program for the Refinement of Crystal Structure*; University of Göttingen: Germany, 1993.
29. *International Tables for Crystallography*; Wilson, A. J. C., Ed.; Kluwer: Dordrecht, 1992; Vol. C.
30. Bruno, I. J.; Cole, J. C.; Edgington, P. R.; Kessler, M. K.; Macrae, C. F.; McCabe, P.; Pearson, J.; Taylor, R. *Acta Crystallogr., Sect. B* **2002**, *58*, 389–397.
31. HYPERCHEM 5.02 Package, Hypercube, Canada, 1997.